

Coherent Random Fiber Laser Based on Nanoparticles Scattering in the Extremely Weakly Scattering Regime

Zhijia Hu,¹ Qun Zhang,^{2,*} Bo Miao,³ Qiang Fu,³ Gang Zou,¹ Yang Chen,² Yi Luo,² Douguo Zhang,³ Pei Wang,³ Hai Ming,³ and Qijin Zhang^{1,†}

¹CAS Key Laboratory of Soft Matter Chemistry, Department of Polymer Science and Engineering, Anhui Key Laboratory of Optoelectronic Science and Technology, University of Science and Technology of China, Hefei, Anhui 230026, China

²Hefei National Laboratory for Physical Sciences at the Microscale and Department of Chemical Physics, University of Science and Technology of China, Hefei, Anhui 230026, China

³Department of Optics and Optical Engineering, University of Science and Technology of China, Hefei, Anhui 230026, China
(Received 31 July 2012; published 18 December 2012)

We demonstrate the realization of a *coherent* random fiber laser (RFL) in the extremely weakly scattering regime, which contains a dispersive solution of polyhedral oligomeric silsesquioxanes nanoparticles (NPs) and laser dye pyromethene 597 in carbon disulfide that was injected into a hollow optical fiber. Multiple scattering of polyhedral oligomeric silsesquioxanes NPs greatly enhanced by the waveguide confinement effect was experimentally verified to account for coherent lasing observed in our RFL system. This Letter extends the NPs-based RFLs from the incoherent regime to the *coherent* regime.

DOI: [10.1103/PhysRevLett.109.253901](https://doi.org/10.1103/PhysRevLett.109.253901)

PACS numbers: 42.55.Zz, 42.55.Mv, 42.55.Wd

Since Letokhov predicted random lasers (RLs) [1], RLs have attracted considerable interest due to their unique properties [2–5]. Compared with conventional lasers requiring a cavity formed by stationary mirrors, RLs only rely on an active medium and a scattering medium, in which an optical feedback is realized by multiple scattering [6–8]. The scattering strength in RLs is evaluated by the scattering mean-free path (l_s) defined as the average distance that light travels between two consecutive scattering events. When the relation of l_s to the sample size L and the wave vector k ($k = 2\pi/\lambda$, λ being the emission wavelength) is taken into account, RLs are generally categorized into three regimes [9]: (i) the localization regime known as the regime for Anderson localization of light, $kl_s \leq 1$ [8]; (ii) the diffusive regime, $\lambda < l_s < L$ [10]; and (iii) the sub-mean-free path regime (or ballistic regime), $L < l_s$ [11]. In a strongly scattering system [12–15], the emergence of coherent random lasing with field or amplitude feedback is generated by interference effects of the scattered waves inside the active medium, which leads to the so-called Anderson localization of light. In a weakly scattering system, RLs with intensity or energy feedback normally feature incoherent lasing behavior, where a narrowed spectral peak can be observed above a threshold [2,16]. Nevertheless, coherent RLs have also been obtained in various weakly scattering systems, such as dye solutions with scattering nanoparticles (NPs) [7,17], polymer films containing silver NPs [18–20], photosensitized polymers incorporating polyhedral oligomeric silsesquioxanes (POSS) NPs [21], and π -conjugated polymers and infiltrated opals [22]. Recently, the effects of two-dimensional confinement on the lasing properties of a classical RL system have received increased attention, bringing

about the birth of random fiber lasers (RFLs) [23]. It is recognized that a RFL system can work in both the incoherent [23] and coherent [24–27] regimes. The hitherto reported coherent RFLs are mainly based on the distributed-feedback mechanism using either randomly distributed Bragg gratings [24,25] or Rayleigh scattering amplified via the Raman effect [26,27]. To date, RFLs based on multiple scattering of NPs in dye solutions have only been found to work in the incoherent regime [23].

Here, we demonstrate *coherent* RFLs based on NPs scattering in the extremely weakly scattering regime. A dispersive solution of POSS NPs and laser dye pyromethene 597 (PM597) in carbon disulfide (CS_2) has been used. When the concentrations of POSS NPs are varied from 24.5 to 1.0 wt %, the corresponding l_s values are determined to be a few tens to hundreds of centimeter, pointing to an extremely weakly scattering regime ($l_s \gg \lambda$). Not surprisingly, *incoherent* RL has been observed for similar samples in a quartz cuvette [28]. Strikingly, however, by *end pumping* a hollow optical fiber filled with the same solution we have achieved *coherent* RFLs under controlled conditions, which is further verified by a power Fourier transform analysis of the emission spectra. By varying the refractive indexes of the liquid core, we demonstrate that the observed coherent random lasing in the extremely weakly scattering regime results from the multiple scattering greatly enhanced by total internal reflection inside our RFL system.

The liquid core optical fiber (LCOF) (10 cm long) was fabricated by filling a solution of POSS NPs (hybrid plastics, size 1–3 nm) and PM597 (laser grade, exciton) in CS_2 into a hollow optical fiber (HOF), the outer (inner) diameter of which is 420 (300) μm . The molecular structures of POSS and PM597 can be found elsewhere [29].

The refractive indexes of the glass cladding of the HOF and CS_2 are 1.514 and 1.627, respectively. The solution was injected into the HOF by capillary force. The optical adhesive was used to seal the LCOF on both ends. The schematic of the entire LCOF system is illustrated in Fig. 1. The 532 nm output of a Q-switched Nd:YAG laser (pulse duration 10 ns, repetition rate 10 Hz) was used to end pump the LCOF system with an f 20 cm focusing lens. The pump pulse energy was controlled by a Glan prism. The emitted light along the LCOF axis was collected by a fiber spectrometer (QE65000, ocean optics, resolution ~ 0.4 nm, integration time 100 ms) after a 560 nm long-wave-pass filter.

Figure 2(a) shows the evolution of emission spectra recorded for the solution of POSS (11.3 wt%) and PM597 (1.47 mM [30]) in CS_2 in a quartz cuvette (1.0 cm long, 1.0 cm wide, and 4.5 cm high) at different pump energies. At low pump energies, only a broad spontaneous emission profile centered at ~ 586 nm was observed, whose full-width-half-maximum (FWHM) is ~ 40 nm. At pump energies above a threshold of ~ 1.12 mJ, a narrowed emission peak (centered at ~ 605 nm, FWHM ~ 4 nm) emerged on top of the broad emission. Such a narrowed spectral feature indicates the incoherent lasing resonances in random lasing media [2]. Figure 2(b) exhibits the evolution of emission spectra recorded for the LCOF system containing the same solution at different pump energies. Remarkably, multimode lasing was observed with multiple sharp peaks above a threshold of ~ 0.41 mJ, whose FWHM is reduced to a large extent (e.g., ~ 0.9 nm for the 606 nm peak at ~ 0.89 mJ). Typically, such a set of sharp spectral features indicates coherent lasing resonances [2,29,31]. To quantitatively describe the degree of spatial coherence we have performed a Young-type double-slit experiment. From the interference fringe data collected on the LCOF system with 11.3 wt% POSS NPs, the spatial coherence function γ is determined to be ~ 0.1 . Figure 2(c) plots the main-peak and integrated emission intensities as a function of the pump energy for the two systems [32]. For both systems, the main-peak intensities turn out to increase rapidly above threshold. However, the threshold for the LCOF system (~ 0.41 mJ) is lower than that for the cuvette system (~ 1.12 mJ). If the coupling loss is reduced, the former

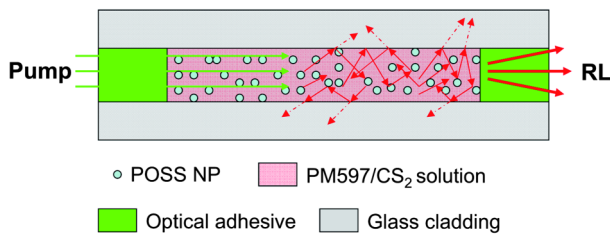


FIG. 1 (color online). Schematic of our LCOF system with the RFL principle based on the waveguide confinement effect illustrated.

will be further decreased. It is known that the “sharpness” of the laser threshold is governed by the β value, which defines the fraction of spontaneous radiation that contributes to lasing. For $0 < \beta < 1$ there is a threshold which

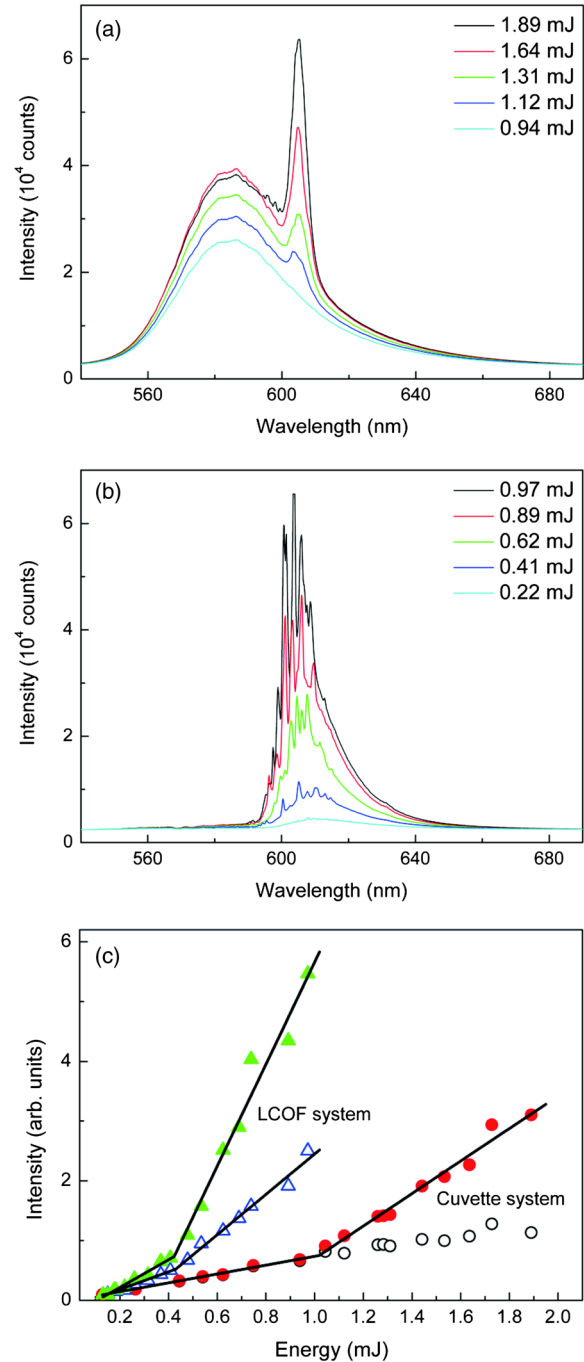


FIG. 2 (color online). The evolution of emission spectra of PM597 (1.47 mM) solutions with 11.3 wt% POSS NPs in CS_2 at different pump energies, which are recorded in (a) the cuvette system and (b) the LCOF system. [For both cases, the spectral intensity increases with increasing the pump energy.] (c) Dependence of the main-peak intensities (solid symbols) as well as the integrated emission intensities (open symbols) on the pump energies, with circles and triangles for (a) and (b), respectively.

becomes sharper as β gets smaller [33]. Unlike the cuvette system, the LCOF system evidently possesses a threshold even if the emission intensity is integrated over its spectrum [Fig. 2(c)]. Such a threshold behavior pointing to a small β value is basically indicative of the directionality of RFLs [23,33–35]. In contrast, conventional RLs usually have considerably large β values and hence lack directionality. The divergence angle of the LCOF output beam was measured to be $\sim 7^\circ$, similar to that reported in Ref. [7]. This observation echoes well to the aforementioned spatial coherence measurement ($\gamma \approx 0.1$). As expected, the degree of directionality of the LCOF system is certainly lower than that of conventional lasers with high spatial coherence. The scattering cross section (at ~ 606 nm) of POSS NPs (particle density $\sim 1.02 \times 10^{20} \text{ cm}^{-3}$) is estimated to be $\sim 3.63 \times 10^{-22} \text{ cm}^2$ [36], corresponding to an l_s of ~ 27 cm. Thus, the cuvette system cannot provide *coherent* feedback into discrete lasing modes as $l_s \gg \lambda$.

Displayed in Fig. 3 are the normalized emission spectra recorded for the LCOF system with different wt % POSS NPs at ~ 0.73 mJ. Only amplified spontaneous emission (FWHM ~ 19 nm) centered at ~ 610 nm was observed when the POSS NPs are absent [Fig. 3(a)]. When varying the wt % of POSS from 1.0 to 24.5 [Figs. 3(b)–3(e)], we observed the characteristic sharp coherent RL features on top of a globally

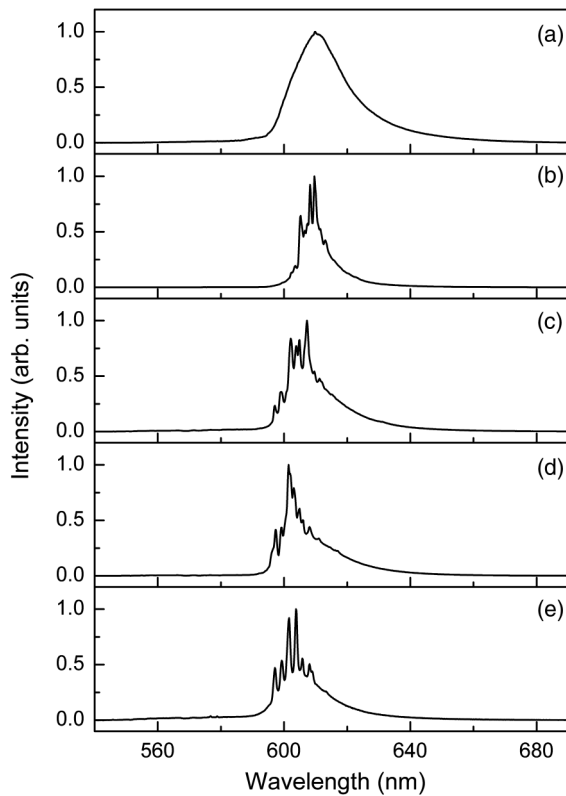


FIG. 3. The normalized emission spectra recorded for the LCOF system with different wt % of POSS at a pump energy of ~ 0.73 mJ: (a) 0.0, (b) 1.0, (c) 11.3, (d) 18.5, and (e) 24.5.

narrowed emission profile. With increasing the wt % of POSS, the main peak was found to gradually blueshift with respect to that without POSS [Fig. 3(a)]. There occurs an ~ 8 nm shift for the 24.5 wt % case [Fig. 3(e)]. To interpret such an observation, we take into account the fact that l_s is inversely proportional to the wt % of POSS while proportional to wavelength [36,37]. More concentrated POSS NPs and shorter wavelengths lead to shorter l_s , increasing the number of scattering events and consequently a longer (and more random) total path in the LCOF system. The blueshift effect [37] observed here can be understood by considering the fact that shorter wavelengths are more amplified than larger wavelengths, and the originally nonlasing shorter wavelengths at low POSS concentrations should also lase preferentially with POSS concentration increasing. Obviously, such a blueshift does not provide much wavelength tunability. Nevertheless, it is possible that the ability to control the emission wavelength can be extended by varying doped nanoparticles with controllable scattering mean-free path and/or by using mixed dyes (see, e.g., Ref. [22]).

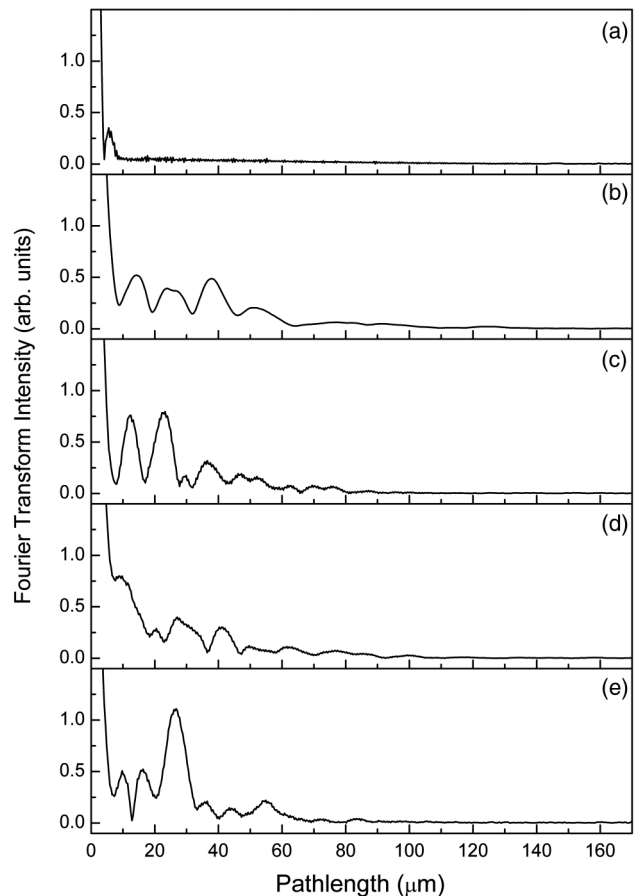


FIG. 4. The power Fourier transform (PFT) of the corresponding emission spectra shown in Fig. 3.

To gain further insight into the excited random cavities of our LCOF system, we have performed a power Fourier transform (PFT) analysis for the emission spectra, as shown in Fig. 4. The PFT of the emission spectrum (in k space) from a well-defined laser cavity yields peaks at Fourier components $p_m = mnL_c/\pi$, where m is the order of the Fourier harmonic, n the refractive index of the gain medium, and L_c the cavity path length [38]. Obviously, sharp lines in the emission spectrum lead to well-separated peaks in the PFT spectrum [Figs. 4(b)–4(e)]. Based on the above relation and $n = 1.627$ for CS_2 , the first sharp peaks in the PFT spectra (i.e., the fundamental Fourier component $m = 1$) give the L_c values of ~ 35.2 , 31.0 , 18.8 , and $18.8 \mu\text{m}$, corresponding to the 1.0, 11.3, 18.5, and 24.5 wt% POSS cases, respectively. However, the corresponding l_s values in the cuvette system are 305.1, 27.0, 16.5, and 12.5 cm, respectively, which are much larger than the corresponding L_c values. If l_s is assumed to be roughly the same for both systems, there should occur only a very small amount of multiple scattering events in the excited random cavities of the LCOF system. Evidently, this is not the case because coherent random lasing was observed even in the case of 1.0 wt% POSS [Fig. 3(b)]. In other words, the l_s values of our LCOF system must have been greatly reduced for some reason. The mechanism responsible for such a great reduction of l_s is most likely related to the waveguide confinement effect provided by the LCOF configuration.

To verify this hypothesis, we have performed controlled experiments, in which the refractive indexes of liquid core (n_{lc}) were varied to examine its influence on the lasing behavior. Figure 5 shows the representative emission spectra recorded with different n_{lc} values for the 24.5 wt% POSS case at ~ 0.81 mJ. The variation of n_{lc} was achieved by adjusting the ratios of ethanol to CS_2 based on $n_{lc} = xn_1 + (1-x)n_2$ [39], where $n_1(n_2)$ is the refractive index

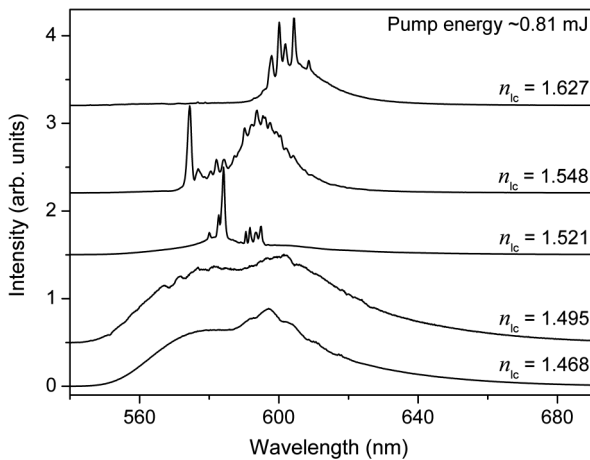


FIG. 5. The emission spectra for the LCOF system containing a solution of 1.47 mM PM597 and 24.5 wt% POSS NPs with different refractive indexes of liquid core.

of ethanol (CS_2) and x the volume ratio of ethanol. Indeed, we observed coherent features when the n_{lc} values are larger than the refractive index of the glass cladding (~ 1.514), satisfying the total internal reflection (TIR) condition. On the contrary, however, these features disappeared when $n_{lc} < 1.514$. This clearly indicates that TIR plays a key role in generating coherent random lasing in the LCOF system. The satisfaction of the TIR condition increases the probability of backscattering of the emitted photons as well as the random total path inside the system. The loop of scattering-TIR-scattering certainly leads to the increase of scattering events (or the decrease of l_s), and hence much larger confinement of emitted photons in the LCOF system (Fig. 1) than in the cuvette system. The greatly enhanced multiple scattering by waveguide confinement effect eventually boosts the probability of light interferences, giving rise to the observed coherent RL behavior in our LCOF system.

In light of the unique feedback mechanism using disorder-induced light scattering, NPs-based RFLs, as demonstrated in the present work, do not require sophisticated laser cavities indispensable for conventional fiber lasers, and hence are free of spatial hole burning that is responsible for shaping the population inversion in standing-wave laser cavities [40]. Admittedly, RFLs are normally inferior to other fiber laser sources such as photonic-crystal fiber lasers [41] in achieving high-power outputs. Furthermore, relatively low spatial coherence as compared to other fiber lasers renders RFLs ideal for speckle-free, full-field laser imaging applications [42] because high spatial coherence may result in coherent imaging artifacts due to the interference occurring during image formation.

To summarize, we have reported a *coherent* random fiber laser based on nanoparticles scattering in the extremely weakly scattering regime. Based on well-designed control experiments combined with pertinent analyses, its working mechanism has been well elucidated; i.e., multiple scattering of nanoparticles in the liquid core optical fiber is greatly enhanced by the waveguide confinement effect under the total internal reflection condition. We envision that the coherent random fiber laser demonstrated in this work may open a window to future random laser applications aiming at low threshold, directionality, and wavelength tunability.

This work was supported by the National Natural Science Foundation of China (Grants No. 21074123, No. 91027024, No. 50973101, No. 21173205, and No. 91127042), the National Basic Research Program of China (Grant No. 2010CB923300), and the Chinese Academy of Sciences (Grant No. XDB01020000). Partial support from the FRFCUC (Grant No. WK2340000012) and the USTC-NSRL Joint Funds (Grant No. KY2340000021) is also acknowledged.

*qunzh@ustc.edu.cn

†zqjm@ustc.edu.cn

- [1] V. S. Letokhov, *JETP Lett.* **5**, 212 (1967).
- [2] H. Cao, *Wave Random Media* **13**, R1 (2003).
- [3] D. S. Wiersma, *Nat. Phys.* **4**, 359 (2008).
- [4] S. Gottardo, R. Sapienza, P. D. García, A. Blanco, D. S. Wiersma, and C. López, *Nat. Photonics* **2**, 429 (2008).
- [5] A. Tulek, R. C. Polson, and Z. V. Vardeny, *Nat. Phys.* **6**, 303 (2010).
- [6] M. P. Van Albada and A. Lagendijk, *Phys. Rev. Lett.* **55**, 2692 (1985).
- [7] X. Wu, W. Fang, A. Yamilov, A. A. Chabanov, A. A. Asatryan, L. C. Botten, and H. Cao, *Phys. Rev. A* **74**, 053812 (2006).
- [8] H. Cao, Y. G. Zhao, S. T. Ho, E. W. Seelig, Q. H. Wang, and R. P. H. Chang, *Phys. Rev. Lett.* **82**, 2278 (1999).
- [9] D. S. Wiersma and A. Lagendijk, *Phys. Rev. E* **54**, 4256 (1996).
- [10] W. L. Zhang, N. Cue, and K. M. Yoo, *Opt. Lett.* **20**, 961 (1995).
- [11] B. R. Prasad, H. Ramachandran, A. K. Sood, C. K. Subramanian, and N. Kumar, *Appl. Opt.* **36**, 7718 (1997).
- [12] A. L. Burin, M. A. Ratner, H. Cao, and R. P. H. Chang, *Phys. Rev. Lett.* **87**, 215503 (2001).
- [13] S. Takeda and M. Obara, *Appl. Phys. B* **94**, 443 (2009).
- [14] N. M. Lawandy, R. M. Balachandran, A. S. L. Gomes, and E. Sauvain, *Nature (London)* **368**, 436 (1994).
- [15] H. E. Türeci, L. Ge, S. Rotter, and A. D. Stone, *Science* **320**, 643 (2008).
- [16] A. M. Brito-Silva, A. Galembek, A. S. L. Gomes, A. J. Jesus-Silva, and C. B. De Araújo, *J. Appl. Phys.* **108**, 033508 (2010).
- [17] S. Mujumdar, M. Ricci, R. Torre, and D. S. Wiersma, *Phys. Rev. Lett.* **93**, 053903 (2004).
- [18] X. G. Meng, K. Fujita, S. Murai, and K. Tanaka, *Phys. Rev. A* **79**, 053817 (2009).
- [19] We also noticed that lasing action has been very recently reported for random metamaterials of metallic nanoparticles [20].
- [20] V. Yannopapas and I. E. Psarobas, *J. Opt.* **14**, 035101 (2012).
- [21] L. Cerdán, A. Costela, I. García-Moreno, O. García, and R. Sastre, *Opt. Express* **18**, 10247 (2010).
- [22] R. C. Polson, A. Chipouline, and Z. V. Vardeny, *Adv. Mater.* **13**, 760 (2001).
- [23] C. J. S. de Matos, L. de S. Menezes, A. M. Brito-Silva, M. A. M. Gámez, A. S. L. Gomes, and C. B. de Araújo, *Phys. Rev. Lett.* **99**, 153903 (2007).
- [24] N. Lizárraga, N. P. Puente, E. I. Chaikina, T. A. Leskova, and E. R. Méndez, *Opt. Express* **17**, 395 (2009).
- [25] M. Gagné and R. Kashyap, *Opt. Express* **17**, 19067 (2009).
- [26] S. K. Turitsyn, S. A. Babin, A. E. El-Taher, P. Harper, D. V. Churkin, S. I. Kablukov, J. D. Ania-Castañón, V. Karalekas, and E. V. Podivilov, *Nat. Photonics* **4**, 231 (2010).
- [27] D. V. Churkin, S. A. Babin, A. E. El-Taher, P. Harper, S. I. Kablukov, V. Karalekas, J. D. Ania-Castañón, E. V. Podivilov, and S. K. Turitsyn, *Phys. Rev. A* **82**, 033828 (2010).
- [28] A. Costela, I. Garcia-Moreno, L. Cerdan, V. Martin, O. Garcia, and R. Sastre, *Adv. Mater.* **21**, 4163 (2009).
- [29] Z. Hu, H. Zheng, L. Wang, X. Tian, T. Wang, Q. Zhang, G. Zou, Y. Chen, and Q. Zhang, *Opt. Commun.* **285**, 3967 (2012).
- [30] The absorption length at 532 nm is estimated to be $\sim 10 \mu\text{m}$ via transmission measurement of the neat dye solution at this concentration. This is smaller than the scattering mean-free path (on the centimeter length scale), which means the pump light will not be scattered out of the system before being absorbed.
- [31] X. Zhao, Z. Wu, S. Ning, S. Liang, D. Wang, and X. Hou, *Opt. Express* **19**, 16126 (2011).
- [32] Note that the data derived from 17 and 16 spectral profiles for the cuvette and LCOF measurements, respectively, are given in Fig. 2(c), while only 5 representative spectral profiles are displayed in Figs. 2(a) and 2(b).
- [33] G. van Soest and A. Lagendijk, *Phys. Rev. E* **65**, 047601 (2002).
- [34] A. L. Burin, M. A. Ratner, H. Cao, and S. H. Chang, *Phys. Rev. Lett.* **88**, 093904 (2002).
- [35] M. P. van Exter, G. Nienhuis, and J. P. Woerdman, *Phys. Rev. A* **54**, 3553 (1996).
- [36] X. H. Wu, A. Yamilov, H. Noh, H. Cao, E. W. Seelig, and R. P. H. Chang, *J. Opt. Soc. Am. B* **21**, 159 (2004).
- [37] A. Veltri, M. Infusino, S. Ferjani, A. De Luca, and G. Strangi, *Phys. Rev. E* **83**, 041711 (2011).
- [38] R. C. Polson, G. Levina, and Z. V. Vardeny, *Appl. Phys. Lett.* **76**, 3858 (2000).
- [39] X. Meng, K. Fujita, S. Murai, J. Konishi, M. Mano, and K. Tanaka, *Opt. Express* **18**, 12153 (2010).
- [40] J. J. Zayhowski, *Opt. Lett.* **15**, 431 (1990).
- [41] J. C. Knight, *J. Opt. Soc. Am. B* **24**, 1661 (2007).
- [42] B. Redding, M. A. Choma, and H. Cao, *Nat. Photonics* **6**, 355 (2012).